Inorganic Chemistry
Communication

Inorg. Chem. **2009**, *48*, 5617–5619 **5617**
DOI: 10.1021/ic900879d

Octacyanometalate-Based Ferrimagnetic $M^{V}Mn^{III}$ (M = Mo, W) Bimetallic Chain Racemates with Slow Magnetic Relaxations

Houng Sik Yoo,[†] Hyun Hee Ko,[†] Dae Won Ryu,[†] Jin Wuk Lee,[†] Jung Hee Yoon,[†] Woo Ram Lee,[†] Hyoung Chan Kim,[‡] Eui Kwan Koh,[§] and Chang Seop Hong*[,†]

[†]*Department of Chemistry (BK21), Korea University, Seoul 136-713, Korea,* [‡]*National Fusion Research Institute, Daejeon 305-333, Korea, and* [§]*Nano-Bio System Research Team, Korea Basic Science Institute, Seoul 136-713, Korea*

Received May 6, 2009

Cyanide-bridged $M^{V}-Mn^{III}$ (M = Mo, W) bimetallic chain complexes with racemic spatial dispositions were constructed by self-assembling $[M(CN)_8]^{3-}$ precursors and Mn^{III} Schiff bases. Antiferromagnetic couplings between spin centers within a chain result in a ferrimagnetic nature, and slow magnetic relaxations are observed as well.

Within the field of molecular magnets, recent advances in single-molecule magnets (SMMs) and single-chain magnets (SCMs) have been well-recognized because of their potential applications in magnetic devices.[1] These developments have fueled research on low-dimensional anisotropic magnetic systems. To attain such anisotropic materials, it is essential to choose effective molecular precursors. Compared to 3d−3d families, 4d, 5d−3d magnetic analogues are known to become more strongly correlated systems because the more diffuse magnetic orbitals of 4d or 5d can promote magnetic coupling rather than the 3d orbital. Some magnetically anisotropic 4d, 5d−3d complexes with cyanide ligands have been prepared by utilizing blocked 4d or 5d molecular building units and exhibited SMM or SCM properties.[2] Special attention to octacyanometalates $[M(CN)_8]^{n-}$ containing 4d or 5d paramagnetic metal ions should be paid because of not only their diffuse orbitals of 4d or 5d and diverse coordination fashions but also because of their photoresponsive properties.[3] To create magnetic anisotropic systems with these octacoordinated building blocks, Mn^{III}(tetradentate Schiff bases) complexes with strong uniaxial magnetic anisotropy are frequently introduced.[4] A few octacyanometalate-based examples have been achieved to date, displaying ferromagnetic or antiferromagnetic characters depending on the Mn Schiff bases used.[5] To realize intriguing anisotropic properties such as slow magnetic relaxation, a new type of magnetic coordination material is highly sought.

We report the syntheses, structures, and magnetic properties of two one-dimensional (1D) chains, $[Mn(5\text{-}Clsalen)(H_2O)(MeOH)]\{[Mn(5\text{-}Clsalen)(H_2O)][Mn(5\text{-}Clsalen)Mo(CN)_8]\}\cdot 3H_2O$ (**1**) [5-clsalen = N,N′-ethylenebis(5-chlorosalicylideneiminato) dianion] and $[Mn(5\text{-}Brsalen)(H_2O)_2]\{[Mn(5\text{-}Brsalen)(H_2O)][Mn(5\text{-}Brsalen)W(CN)_8]\}\cdot H_2O\cdot 3MeOH$ (**2**), formed by octacyanometalate(V) anions and anisotropic Mn^{III} Schiff base cations. These compounds mark unique $M^{V}Mn^{III}$ (M = Mo, W) chain structures with racemic spatial arrangements, exhibiting ferrimagnetic natures and slow magnetic relaxations.

A stoichiometric reaction of $(HBu_3N)_3[Mo(CN)_8]$ in $MeOH/H_2O$ (5:1) or $(Bu_4N)_3[W(CN)_8]$ in MeOH with corresponding Mn Schiff bases in MeOH yielded brown crystals of both complexes. The reaction progress was checked by inspecting the CN peaks in the IR spectra. The characteristic CN stretching vibrations are observed at 2142w cm^{-1} for

*To whom correspondence should be addressed. E-mail: cshong@korea.ac.kr.

(1) (a) Gatteschi, S.; Sessoli, R. *Angew. Chem., Int. Ed.* **2003**, *42*, 268. (b) Lescouëzec, R.; Toma, L. M.; Vaissermann, J.; Verdaguer, M.; Delgado, F. S.; Ruiz-Pérez, C.; Lloret, F.; Julve, M. *Coord. Chem. Rev.* **2005**, *249*, 2691. (c) Coulon, C.; Miyasaka, H.; Clérac, R. *Struct. Bonding (Berlin)* **2006**, *122*, 163.

(2) (a) Sokol, J. J.; Hee, A. G.; Long, J. R. *J. Am. Chem. Soc.* **2002**, *124*, 7656. (b) Schelter, E. J.; Prosvirin, A. V.; Dunbar, K. R. *J. Am. Chem. Soc.* **2004**, *126*, 15004. (c) Yoon, J. H.; Lim, J. H.; Kim, H. C.; Hong, C. S. *Inorg. Chem.* **2006**, *45*, 9613. (d) Choi, S. W.; Kwak, H. Y.; Yoon, J. H.; Kim, H. C.; Koh, E. K.; Hong, C. S. *Inorg. Chem.* **2008**, *47*, 10214. (e) Song, Y.; Zhang, P.; Ren, X.-M.; Shen, X.-F.; Li, Y.-Z.; You, X.-Z. *J. Am. Chem. Soc.* **2005**, *127*, 3708. (f) Lim, J. H.; Yoon, J. H.; Kim, H. C.; Hong, C. S. *Angew. Chem., Int. Ed.* **2006**, *45*, 7424.

(3) (a) Arimoto, Y.; Ohkoshi, S.-i.; Zhong, Z. J.; Seino, H.; Mizobe, Y.; Hashimoto, K. *J. Am. Chem. Soc.* **2003**, *125*, 9240. (b) Herrera, J. M.; Marvaud, V.; Verdaguer, M.; Marrot, J.; Kalisz, M.; Mathoniere, C. *Angew. Chem., Int. Ed.* **2004**, *43*, 5468.

(4) (a) Miyasaka, H.; Saitoh, A.; Abe, S. *Coord. Chem. Rev.* **2007**, *251*, 2622. (b) Kwak, H. Y.; Ryu, D. W.; Kim, H. C.; Koh, E. K.; Cho, B. K.; Hong, C. S. *Dalton. Trans.* **2009**, 1954. (c) Yoon, J. H.; Ryu, D. W.; Kim, H. C.; Yoon, S. W.; Suh, B. J.; Hong, C. S. *Chem.—Eur. J.* **2009**, *15*, 3661.

(5) (a) Przychodzeń, P.; Rams, M.; Guyard-Duhayon, C.; Sieklucka, B. *Inorg. Chem. Commun.* **2005**, *8*, 350. (b) Kou, H.-Z.; Ni, Z.-H.; Zhou, B. C.; Wang, R.-J. *Inorg. Chem. Commun.* **2004**, *7*, 1150. (c) Przychodzeń, P.; Lewiński, K.; Bałanda, M.; Pełka, R.; Rams, M.; Wasiutyński, T.; Guyard-Duhayon, C.; Sieklucka, B. *Inorg. Chem.* **2004**, *43*, 2967. (d) Ko, H. H.; Lim, J. H.; Yoo, H. S.; Kang, J. S.; Kim, H. C.; Koh, E. K.; Hong, C. S. *Dalton Trans.* **2007**, 2061.

Published on Web 06/03/2009

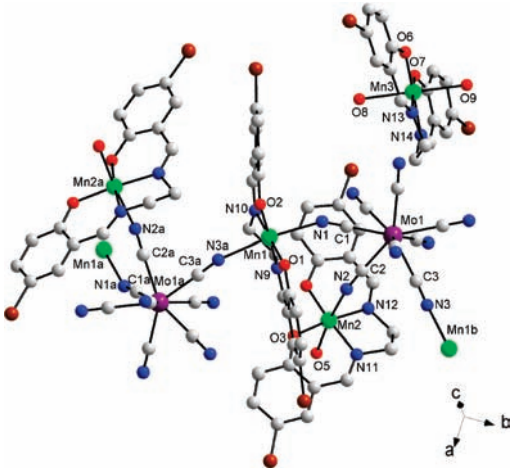

Figure 1. Molecular view of **1** with selected atom-labeling scheme. Symmetry transformations used to generate equivalent atoms: $a = 1 - x$, $-0.5 + y$, $0.5 - z$ and $b = 1 - x$, $0.5 + y$, $0.5 - z$.

$(HBu_3N)_3[Mo(CN)_8]$ and 2148w cm^{-1} for **1**, while the peaks are visible at 2131w cm^{-1} for $(Bu_4N)_3[W(CN)_8]$ and 2156w cm^{-1} for **2**. It is evident that the bands in the products move toward higher frequencies with respect to the peaks of the starting octacyanometalates, which definitely indicates the binding of the N ends of the CN ligands to Mn(III) centers.

Two complexes are nearly isostructural, and the structure of **1** is illustrated in Figure 1 as a representative molecular view (**2** in Figure S1, Supporting Information). The M center (M = Mo, W) is encircled by eight CN groups. We performed a continuous shape measures analysis to determine the exact geometry around the central atoms, which is informative because the magnetic exchange coupling is governed by the surroundings of the metal centers in octacyanometalate(V)-based magnetic materials.[6,7] The S_X (X = SAPR, DD, BTP) values against ideal symmetry of a square antiprism (SAPR, D_{4d}), a dodecahedron (DD, D_{2d}), and a bicapped trigonal prism (BTP, C_{2v}) are summarized in Table S1 (Supporting Information). On the basis of the obtained values, it is manifest that the environment of M belongs to a distorted SAPR. The small value of Δ demonstrates that the actual polyhedral shape is subject to the interconversion path between SAPR and DD. The average M−C distances are 2.15(3) Å for **1** and 2.15(2) Å for **2**, and the M−C−N angles are slightly away from linearity with a maximum deviation of 3.8° for **1** and 3.5° for **2**. For the Mn(III) units in a chain, a typical Jahn−Teller distortion is revealed, as judged by the more elongated axial Mn−N lengths (Mn1−N1 = 2.358(6) Å, Mn1b−N3=2.340(6) Å, Mn2−N2 = 2.317(5) Å for **1**; Mn1−N1=2.308(8) Å, Mn1d−N3=2.339(7) Å, Mn2−N2 = 2.326(8) Å for **2**; $b = 1 - x$, $0.5 + y$, $0.5 + z$ and $d = 1 - x$, $-0.5 + y$, $0.5 - z$) compared to the equatorial Mn−N(O) lengths of about 1.93 Å for **1** and **2**. The magnetically important Mn−N−C angles in the bridging pathways are 151.6(6)° for Mn1−N1−C1, 155.6(5)° for Mn1b−N3−C3, and 155.7(6)° for Mn2−N2−C2 (**1**) as well as 154.7(6)° for Mn1−N1−C1, 149.5(7)° for Mn1d−N3−C3, and 155.3(7)° for Mn2−N2−C2 (**2**).

The overall structure of **1** in the *ab* plane shows that chains are well-separated from each other in the *a* direction by isolated Mn Schiff bases (Figure S2, Supporting Information). Chains running along the *b* axis are interconnected by hydrogen bonds among coordinated oxygens, phenoxide oxygens, and nitrogens of free CN ligands with a distance range of 2.717−2.807 Å, as well as $\pi-\pi$ stacking forces between phenoxide rings related to Mn3 on adjacent chains (centroid distance = 3.651 Å), subsequently forming a two-dimensional array. The isolated Mn Schiff bases are dimerized by hydrogen bonds with a distance of 2.897 Å. A similar structural aspect is also disclosed in **2** with slightly short intermolecular contacts (Figure S3, Supporting Information). The anionic 1D chain is constructed by the self-assembly of $[Mo(CN)_8]^{3-}$ and two types of $[Mn(5\text{-}Clsalen)]^{+}$ moieties. It is interesting to note that the backbone of the chain is formed by a 1:1 adduct of the octacyanometalates and Mn Schiff bases and additionally branched by another Mn Schiff base. Notably, this structural pattern is unique among octacyanometalate-linked $M^{V}Mn^{III}$ magnetic assemblies, although this kind of zigzag chain with one additional metal center dangling on the side has been observed for some $Mo^{IV}(Nb^{IV})-Mn^{II}$ compounds.[5,8] The intrachain M−Mn distances are in the range from 5.432 to 5.514 Å for **1** and from 5.472 to 5.498 Å for **2**. The separations between M and Mn3 are 7.593 Å for **1** and 7.505 Å for **2**. Interestingly, each chain designates helicity with a long pitch of 15.856 Å for **1** and 15.698 Å for **2**. *P*- and *M*-helical chains in **1** and **2** are stacked in a heterochiral manner, finally generating a racemate (Figures S4 and S5, Supporting Information). This racemic trait is normally perceived in systems built by not only archiral but also chiral ligands.[9]

The magnetic susceptibility data for **1** and **2** were collected at 1000 G in the temperature range of 2−300 K, as plotted in Figure 2 and Figure S6 (Supporting Information). The $\chi_m T$ values at 300 K are 9.26 cm^3 K mol^{-1} (**1**) and 9.24 cm^3 K mol^{-1} (**2**), which are somewhat smaller than the spin-only one (9.375 cm^3 K mol^{-1}) anticipated for a noncoupled M(V) ($S_M = 1/2$) and three noncoupled Mn(III) ($S_{Mn} = 2$) spins. As the temperature is lowered, $\chi_m T$ undergoes a gradual reduction and goes down to a minimum of 8.53 cm^3 K mol^{-1} at $T_{min} = 8$ K for **1** and 8.81 cm^3 K mol^{-1} at $T_{min} = 40$ K for **2**. Below T_{min}, $\chi_m T$ starts to increase, reaching a peak at 7 K for **1** and 9 K for **2**. This magnetic behavior is associated with a ferrimagnetic nature arising from an antiferromagnetic consequence between M(V) and Mn(III) spins in a chain. Eventually, a drastic drop in the $\chi_m T(T)$ plot occurs right below the cusp temperature, which may be relevant to zero-field splittings or interchain magnetic interactions. The magnetic data at $T > 9$ K (**1**) and $T > 40$ K (**2**) were fitted with the Curie−Weiss law [$\chi_m = C/(T - \theta)$], leading to $C = 9.30$ cm^3 K mol^{-1} and $\theta = -1.2$ K for **1** and $C = 9.32$ cm^3 K mol^{-1} and $\theta = -2.9$ K for **2**. The negative θ terms demonstrate that neighboring magnetic centers are antiferromagnetically coupled.

(6) Llunell, M.; Casanova, D.; Cirera, J.; Bofill, J. M.; Alemany, P.; Alvarez, S.; Pinsky, M.; Avnir, D. *SHAPE*, v1.1b; University of Barcelona: Barcelona, Spain, 2005.

(7) Visinescu, D.; Desplansches, C.; Imaz, I.; Bahers, V.; Pradhan, R.; Villamena, F. A.; Guionneau, P.; Sutter, J.-P. *J. Am. Chem. Soc.* **2006**, *128*, 10202.

(8) (a) Rombaut, G.; Golhen, S.; Ouahab, L.; Mathoniere, C.; Kahn, O. *J. Chem. Soc., Dalton Trans.* **2000**, 3609. (b) Pradhan, R.; Desplanches, C.; Guionneau, P.; Sutter, J.-P. *Inorg. Chem.* **2003**, *42*, 6607.

(9) (a) Tabellion, F. M.; Seidel, S. R.; Arif, A. M.; Stang, P. J. *Angew. Chem., Int. Ed.* **2001**, *40*, 1529. (b) Yoo, H. S.; Kim, J. I.; Yang, N.; Koh, E. K.; Park, J.-G.; Hong, C. S. *Inorg. Chem.* **2007**, *46*, 9054.

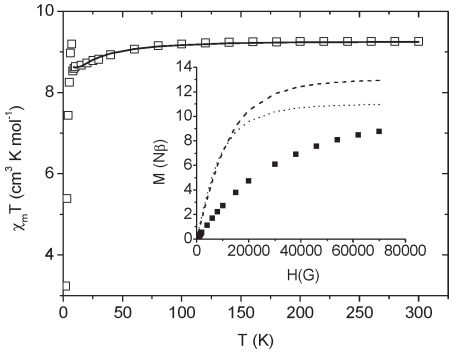

Figure 2. Plot of $\chi_m T$ versus T for **1**. The solid line in the main panel shows the best fit to the magnetic model. The inset represents the $M(H)$ data and the Brillouin curves calculated from $S_{Mo} + 3S_{Mn}$ (dashed line) and $S_{trimer} + S_{Mn}$ (dotted line).

To probe the magnetic exchange coupling between spin centers, we examined the magnetically related structural parameters. For **1**, the bond lengths of Mn−N in the bridging routes are almost alike, but among them the Mn1−N1 distance is longest. Moreover, the bridging angles of Mn2−N2−C2 and Mn1b−N3−C3 are nearly identical, while the Mn1−N1−C1 angle is fairly acute, by 4°, against the other angles. With reference to the related structural data, we reasonably assumed that the Mn2−N≡C−Mo1 and Mn1b−N≡C−Mo1 skeletons communicate stronger magnetic couplings than the Mn1−N≡C−Mo1 path.[10,11] Hence, a suitable approximate magnetic system is devised employing the trinuclear subunit Mn2−Mo1−Mn1b with the spin Hamiltonian $H = -J_t(S_{Mn2}S_{Mo1} + S_{Mo1}S_{Mn1b}) + g\beta H(S_{Mn2} + S_{Mo1} + S_{Mn1b})$. The analogous evaluation of the structural data of **2** allows for the magnetic model of the trinuclear subunit based on $H = -J_t(S_{Mn2}S_{W1} + S_{W1}S_{Mn1}) + g\beta H(S_{Mn2} + S_{W1} + S_{Mn1})$. Application of the Van Vleck formula affords the exact expression of the magnetic susceptibility of the trinuclear unit (χ_t). As given in Figure 3, we adopted an infinite chain model (χ_c) by regarding the trinuclear moiety as a classical spin (S_t).[11d,12] The final magnetic equation (χ_m) is a combination of the chain (χ_c) and paramagnetic contributions (χ_{Mn}) for the isolated Mn(III) ion.

$$\chi_t = (Ng^2\beta^2/3kT)S_t(S_t+1)$$

$$\chi_c = [(Ng^2\beta^2 S_t(S_t+1)/3kT)][(1+u)/(1-u)]$$

$$\chi_m = \chi_c + \chi_{Mn}$$

where $u = \coth(J_c S_t(S_t+1)/kT - kT/J_c S_t(S_t+1)$

A best fit with the experimental data at $T > 9$ K (**1**) and $T > 20$ K (**2**) brings about magnetic parameters of $g = 2.0$, $J_t = -4.0$ cm^{-1}, and $J_c = -0.43$ cm^{-1} for **1** and $g = 2.0$, $J_t = -9.6$ cm^{-1}, and $J_c = -1.0$ cm^{-1} for **2**. The obtained J values

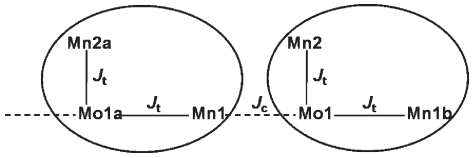

Figure 3. Schematic representation of magnetic exchange couplings in **1**. The solid lines stand for intratimer interactions (J_t) and the dotted ones for intertrimer interactions (J_c).

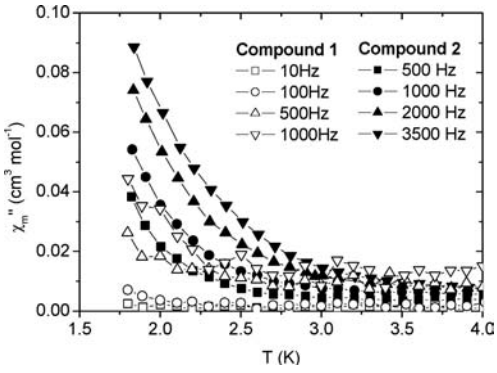

Figure 4. Plot of χ_m'' versus T for **1** and **2** at indicated frequencies.

unveil the operation of antiferromagnetic interactions between M(V) and Mn(III) transmitted by CN linkage and decrease in the range of octacyanometalate-based $M^{V}Mn^{III}$ bimetallic systems.[5] The greater magnetic coupling in **2** compared to that in **1** is due to the fact that the 5d orbital is more diffuse than the 4d orbital in the same SAPR geometry.[7,11]

The field-dependent magnetizations were plotted in the insets of Figure 2 and Figure S6 (Supporting Information), collected at a temperature of 2 K and at fields spanning from 0 to 7 T. The data lie below the calculated Brillouin curves from three independent Mn(III) and one independent M(V) center, or the antiferromagnetically coupled $Mn^{III}M^{V}Mn^{III}$ trinuclear unit and the separated Mn(III) atom. This result points out that dominant antiferromagnetic interactions take place among trimers and monomers.

Figure 4 illustrates the ac susceptibility data taken at several oscillating frequencies. The out-of-phase components (χ_m'') of **1** and **2** are rather frequency-dependent, which suggests the existence of a slowly relaxed magnetized phase, presumably reminiscent of superparamagnetic-like behavior.[1,2] Further analysis of the spin dynamics would be hampered because no maxima were detectable.

In summary, we have prepared and characterized the first structural types of $M^{V}Mn^{III}$ bimetallic chains with spatial racemic features by reacting $[M(CN)_8]^{3-}$ with the respective anisotropic Mn Schiff bases. The ferrimagnetic behavior between two metal centers within a chain is evident in both complexes, and slow magnetic relaxations are observed in the 1D magnetic systems.

Acknowledgment. This work was supported by the Korea Science and Engineering Foundation (KOSEF) grant (No. R01-2007-000-10240-0).

Supporting Information Available: X-ray crystallographic files in CIF format; additional synthetic, structural, and magnetic data for **1** and **2**. This material is available free of charge via the Internet at http://pubs.acs.org.

(10) Kou, H.-Z.; Zhou, B. C.; Liao, D.-Z.; Wang, R.-J.; Li, Y. *Inorg. Chem.* **2002**, *41*, 6887.

(11) (a) Venkatakrishnan, T.; Desplanches, C.; Rajamani, R.; Guionneau, P.; Ducasse, L.; Ramasesha, S.; Sutter, J.-P. *Inorg. Chem.* **2008**, *47*, 4854. (b) Korzeniak, T.; Desplanches, C.; Podgajny, R.; Gimenez-Saiz, C.; Stadnicka, K.; Rams, M.; Sieklucka, B. *Inorg. Chem.* **2009**, *48*, 2865. (c) Lim, J. H.; Kang, J. S.; Kim, H. C.; Koh, E. K.; Hong, C. S. *Inorg. Chem.* **2006**, *45*, 7821. (d) Lim, J. H.; You, Y. S.; Yoo, H. S.; Yoon, J. H.; Kim, J. I.; Koh, E. K.; Hong, C. S. *Inorg. Chem.* **2007**, *46*, 10578.

(12) Kou, H.-Z.; Zhou, B. C.; Gao, S.; Liao, D.-Z.; Wang, R.-J. *Inorg. Chem.* **2003**, *42*, 5604.